LETTER

doi:10.1038/nature09392

Single-shot readout of an electron spin in silicon

Andrea Morello[1], Jarryd J. Pla[1], Floris A. Zwanenburg[1], Kok W. Chan[1], Kuan Y. Tan[1], Hans Huebl[1]†, Mikko Möttönen[1,3,4], Christopher D. Nugroho[1]†, Changyi Yang[2], Jessica A. van Donkelaar[2], Andrew D. C. Alves[2], David N. Jamieson[2], Christopher C. Escott[1], Lloyd C. L. Hollenberg[2], Robert G. Clark[1]† & Andrew S. Dzurak[1]

The size of silicon transistors used in microelectronic devices is shrinking to the level at which quantum effects become important[1]. Although this presents a significant challenge for the further scaling of microprocessors, it provides the potential for radical innovations in the form of spin-based quantum computers[2–4] and spintronic devices[5]. An electron spin in silicon can represent a well-isolated quantum bit with long coherence times[6] because of the weak spin–orbit coupling[7] and the possibility of eliminating nuclear spins from the bulk crystal[8]. However, the control of single electrons in silicon has proved challenging, and so far the observation and manipulation of a single spin has been impossible. Here we report the demonstration of single-shot, time-resolved readout of an electron spin in silicon. This has been performed in a device consisting of implanted phosphorus donors[9] coupled to a metal-oxide-semiconductor single-electron transistor[10,11]—compatible with current microelectronic technology. We observed a spin lifetime of ~6 seconds at a magnetic field of 1.5 tesla, and achieved a spin readout fidelity better than 90 per cent. High-fidelity single-shot spin readout in silicon opens the way to the development of a new generation of quantum computing and spintronic devices, built using the most important material in the semiconductor industry.

The projective, single-shot readout of a qubit is a crucial step in both circuit-based and measurement-based quantum computers[12]. For electron spins in the solid state, this has only been achieved in GaAs/AlGaAs quantum dots coupled to charge detectors[13–15]. The spin readout was achieved using spin-dependent tunnelling, in which the electron was displaced to a different location depending on its spin state. The charge detector, electrostatically coupled to the electron site, sensed whether the charge had been displaced, thereby determining the spin state. Here we apply a novel approach to charge sensing, where the detector is not only electrostatically coupled, but also tunnel-coupled to the electron site[11], as shown in Fig. 1a. The strong coupling inherent to this arrangement is responsible for the high charge transfer signals that ultimately allow fast and high-fidelity single-shot spin readout. As a charge detector, we use here the silicon single-electron transistor[10] (SET), a nonlinear nanoelectronic device consisting of a small island of electrons tunnel-coupled to source and drain reservoirs, electrostatically induced beneath an insulating SiO_2 layer. A current can flow from source to drain only when the electrochemical potential of the island assumes specific values[16], resulting in a characteristic pattern of sharp current peaks as a function of gate voltage (Fig. 1e). The shift in electrochemical potential arising from the tunnelling of a single electron from a nearby charge centre into the SET island is large enough to switch the current from zero to its maximum value. This tunnelling event becomes spin-dependent in the presence of a large externally applied magnetic field B, when the spin-up state $|\uparrow\rangle$ has a higher energy than the spin-down state $|\downarrow\rangle$, by an amount $E_Z = g\mu_B B$, where $g \approx 2$ is the spin gyromagnetic ratio and μ_B is the Bohr magneton. The Zeeman splitting E_Z must be larger than the thermal and electromagnetic broadening of electron states in the SET island. Therefore we perform the experiment in high magnetic fields, $B > 1$ T, and with very low electron temperatures, $T_{el} \approx 200$ mK.

The high effective mass of the conduction electrons and the six-fold degeneracy of the conduction band minima (valleys) in silicon[17] imply that very tight confinement is required to isolate a single electron in a non-degenerate state. A phosphorus atom in silicon naturally provides a sharp confining potential for its bound donor electron. The quantum states $|\uparrow\rangle$, $|\downarrow\rangle$ of the electron spin $S = 1/2$ form a natural qubit, with the additional advantage that the ^{31}P nuclear spin can be used as a long-lived quantum memory[18]. Therefore we have fabricated a batch of devices where P donors were implanted in a small region (90×90 nm) next to the SET (Fig. 1c). The P^+ ion fluence was chosen to maximize the likelihood that three donors are located at a distance ~30–60 nm from the SET island and can be tunnel-coupled to it, forming a parallel double-quantum-dot system[19]. The SET top gate and a plunger gate overlaying the P-implanted area provide full electrostatic control of the hybrid double-dot. Here we present the complete data for one device (A), together with the spin lifetime measurements on another one (B).

To perform spin readout, we bias the gates so as to tune the electrochemical potentials on the SET (μ_{SET}) and a nearby donor ($\mu_\downarrow$ and $\mu_\uparrow$ for states $|\downarrow\rangle$ and $|\uparrow\rangle$, respectively) such that the SET current, I_{SET}, is zero when the electron resides on the donor, while $I_{SET} \neq 0$ when the donor is ionized. The readout protocol consists of three phases[13], shown in Fig. 1b. (1) A 'load' phase, during which an electron in an unknown spin state tunnels from the SET island to the donor, as $\mu_{SET} > \mu_\downarrow, \mu_\uparrow$. The electron loading is signalled by I_{SET} dropping to zero. (2) A 'read' phase, during which a spin-down electron remains trapped on the donor, leaving $I_{SET} = 0$, but a spin-up electron can tunnel onto the SET island, causing $I_{SET} = I_{max}$. A (different) spin-down electron from the SET island can later tunnel back onto the donor, blocking the current again. Therefore, the signal of a state $|\uparrow\rangle$ is a single current pulse at the beginning of the read phase. (3) An 'empty' phase during which the donor is ionized, to ensure that a new electron with random orientation can be loaded at the next cycle.

Measuring I_{SET} as a function of the plunger (V_{pl}) and SET top (V_{top}) gate voltages yields the map shown in Fig. 1d. Each time a charge centre coupled to the SET changes its charge state, the sequence of SET current peaks breaks and shifts in gate voltage by an amount $\Delta V_{top} = \Delta q / C_{top}$, where Δq is the charge induced on the SET island and C_{top} is the capacitance between island and top gate (Fig. 1e). Figure 1d shows a large number of charge transitions for $-0.7 < V_{pl} < 0$ V. Most of these transitions are irreproducible and hysteretic, and are probably caused by the charging/discharging of shallow traps at the Si/SiO_2 interface. The transitions for $V_{pl} < -0.7$ V, however, are stable and well reproduced even after several thermal cycles. Their number is consistent with the expected number of implanted donors in the active area, and they have been observed in a number of similar devices[20].

[1]Australian Research Council Centre of Excellence for Quantum Computer Technology, School of Electrical Engineering and Telecommunications, University of New South Wales, Sydney, New South Wales 2052, Australia. [2]Australian Research Council Centre of Excellence for Quantum Computer Technology, School of Physics, University of Melbourne, Melbourne, Victoria 3010, Australia. [3]Department of Applied Physics/COMP, Aalto University, PO Box 15100, 00076 Aalto, Finland. [4]Low Temperature Laboratory, Aalto University, PO Box 13500, 00076 Aalto, Finland. †Present addresses: Walther-Meissner-Institut, Bayerische Akademie der Wissenschaften, 85748 Garching, Germany (H.H.); Department of Physics, University of Illinois at Urbana-Champaign, Urbana, Illinois 61801, USA (C.D.N.); Department of Defence, Canberra, Australian Capital Territory 2600, Australia (R.G.C.).

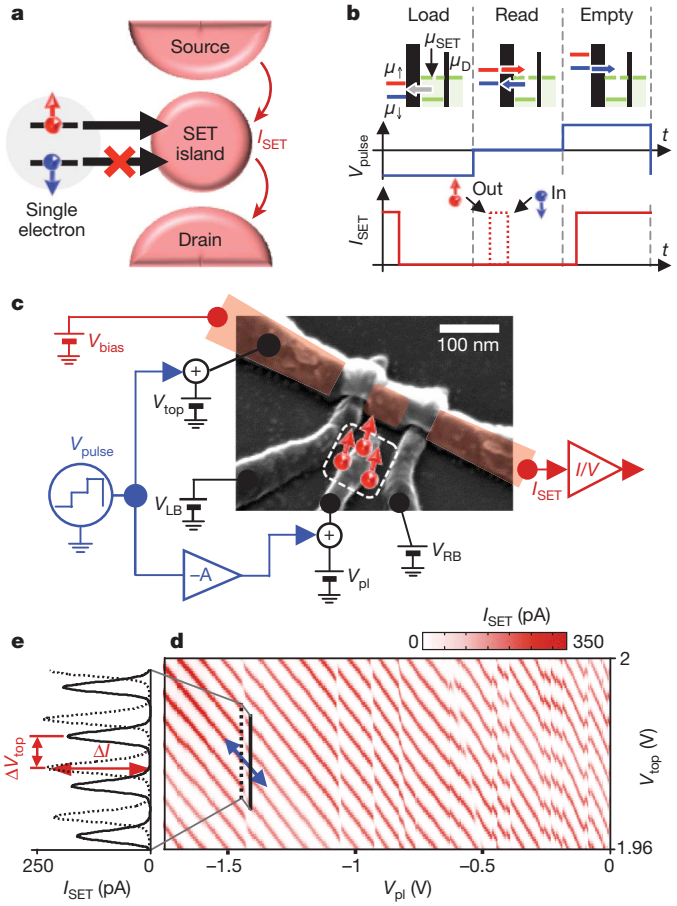

Figure 1 | Spin readout device configuration and charge transitions. **a**, Diagram showing the spin-dependent tunnelling configuration, where a single electron can tunnel onto the island of a SET only when in a spin-up state. **b**, Pulsing sequence for single-shot spin readout (see main text), and SET response, I_{SET}. The dashed peak in I_{SET} is the expected signal from a spin-up electron. The diagrams at the top depict the electrochemical potentials of the electron site ($\mu_{\downarrow,\uparrow}$), of the SET island ($\mu_{SET}$) and of the drain contact (μ_D). **c**, Scanning electron micrograph of a device similar to the one measured. The area where the P donors are implanted is marked by the dashed square. Both d.c. voltages and pulses are applied to the gates as indicated. The red shaded area represents the electron layer induced by the top gate and confined beneath the SiO_2 gate oxide layer. **d**, SET current I_{SET} as a function of the voltages on the top and the plunger gates, V_{top} and V_{pl}, at $B = 0$. The lines of SET Coulomb peaks are broken by charge transfer events. The blue arrow on the transition at $V_{pl} \approx -1.4$ V shows the axis along which V_{top} and V_{pl} are pulsed for compensated time-resolved measurements, ensuring that μ_{SET} remains constant during the pulsing. **e**, Line traces of I_{SET} along the solid and dashed lines in **d**. Ionizing the donor shifts the sequence of SET current peaks by an amount $\Delta V_{top} = \Delta q/C_{top}$, causing a change ΔI in the current. The charging energy of the SET is ~1.5 meV.

Considering the results of the spin lifetime measurements discussed below, it is likely that we are observing transitions between D^+ and D^0 states of implanted P donors[21].

The charge transition at $V_{pl} \approx -1.4$ V in Fig. 1d has a large $\Delta q \approx 0.7e$, where $1e$ is equivalent to the spacing between adjacent current peaks. This indicates a donor very close to the SET island[11]. Accordingly, we find a fast electron tunnelling time between the donor and the SET, of the order of 10 μs. For comparison, the charge transition at $V_{pl} \approx -1.1$ V has a lower $\Delta q \approx 0.3e$ and a much slower tunnel time, ~10 ms, consistent with a donor further away. We chose the donor transition at $V_{pl} \approx -1.4$ V to implement the spin readout protocol. Figure 2b–g illustrates the method we used to find the values of V_{pulse} during the read phase at which spin-dependent tunnelling is achieved. By lowering the read level from too high (Fig. 2c) to too low (Fig. 2g), the time traces of I_{SET} during the read phase show a transition from $I_{SET} = I_{max}$, through random telegraph signal, to $I_{SET} = 0$, passing through a region where I_{SET} can be either zero (Fig. 2e) or show a spin-up signal (Fig. 2f). In this region, the condition $\mu_\downarrow < \mu_{SET} < \mu_\uparrow$ is fulfilled, and a single-shot projective measurement of the electron spin state is performed. When plotting the average of several single-shot traces taken at different read levels, the correct readout range is highlighted by the appearance of a high current region at the beginning of the read phase, spanning a time interval of the order of the electron tunnel time $1/\Gamma$ (Fig. 4). Such a high-current region is absent in measurements performed in zero magnetic field, as expected. With a modified pulse sequence, it is also possible to extract the Zeeman energy splitting, $E_Z = g\mu_B B$, and demonstrate the deterministic loading of a $|\downarrow\rangle$ electron (Supplementary information). Because the loading of a state $|\downarrow\rangle$ is controlled by gate voltages and occurs on ~10-μs timescales as determined by the electron tunnel time, this device already realizes two essential requirements for quantum computation and quantum error correction, namely, single-shot readout and fast preparation of the qubit ground state[22].

Defining $P_\uparrow$ as the probability of observing a spin-up electron, we find that $P_\uparrow$ decreases when increasing the wait time τ_w before the spin is read out (Fig. 3a), because the excited state $|\uparrow\rangle$ relaxes to the ground state $|\downarrow\rangle$. The wait time dependence of $P_\uparrow$ (Fig. 3b, c) is well described by a single exponential decay, $P_\uparrow(\tau_w) = P_\uparrow(0)\exp(-\tau_w/T_1)$, where T_1 is the lifetime of the spin excited state.

The measured spin relaxation rates as a function of magnetic field, $T_1^{-1}(B)$, at phonon temperature $T \approx 40$ mK, are plotted in Fig. 3d. The data on device A for $B \geq 2$ T are well described by the function $T_1^{-1}(B) \approx K_{0A} + K_{5A}B^5$, with $K_{0A} = 1.84 \pm 0.07\ s^{-1}$ and $K_{5A} = 0.0076 \pm 0.0002\ s^{-1}\,T^{-5}$. A fit of the form $T_1^{-1}(B) = K_0 + K_aB^a$, where K_0, K_a and a are free parameters, yields $a = 4.8 \pm 0.2$. The data on device B follow $T_1^{-1}(B) \approx K_{5B}B^5$, with $K_{5B} = 0.015 \pm 0.0005\ s^{-1}\,T^{-5}$ down to $B = 1.5$ T, where the spin lifetime has a value $T_1 = 6 \pm 2$ s. We attribute the B-independent contribution observed in device A to the effect of dipolar coupling between the spin under measurement and those of neighbouring donors (Supplementary Information). This effect depends on the details of the mutual distance between implanted donors, and is therefore strongly sample-dependent. The $T_1^{-1} \propto B^5$ dependence agrees with the low-T limit[23] ($k_BT \ll g\mu_BB$) of a spin–lattice relaxation mechanism arising from valley repopulation[24], that is, the change in the relative weight of the six conduction band minima (valleys) of Si caused by the deformation of the crystal lattice when the state $|\uparrow\rangle$ relaxes to $|\downarrow\rangle$, emitting an acoustic phonon. This is the dominant relaxation channel for donors, where orbital excited states are very high in energy. Conversely, for spins in electrostatically defined quantum dots[23] in silicon, relaxation through low-lying orbital states can lead to $T_1^{-1} \propto B^7$. This dependence has been recently observed in Si/SiGe (ref. 25) and Si/SiO_2 (ref. 26) quantum dots.

Our results are also incompatible with the known relaxation process for interface traps, which is dominated by the coupling to two-level fluctuators[27], yielding $T_1^{-1} \propto B^3$. A recent electron spin resonance experiment on shallow traps at the Si/SiO_2 interface[28] found $T_1 \approx 800$ μs at $T = 350$ mK and $B = 0.32$ T, that is, 2 to 3 orders of magnitude shorter than our result, despite the much lower magnetic field. An experiment on bulk-doped Si:P by conventional electron spin resonance techniques (J. J. L. Morton, personal communication) yielded $T_1 = 0.42$ s at $B = 3.35$ T and $T < 5$ K, that is, in the T-independent regime. This data point is only a factor of ~1.3 below the line $T_1^{-1}(B) \approx K_{5A}B^5$. We conclude that the observation of $T_1^{-1} \propto B^5$ and the quantitative agreement with bulk Si:P data constitute a strong indication that we have measured the spin of a single electron bound to an implanted P donor. The proximity of the donor to electrostatic gates and a Si/SiO_2 interface[29] could be responsible for the slight variability of T_1 (Supplementary Information) but, importantly, does not substantially compromise the long spin lifetime of the donor-bound electron.

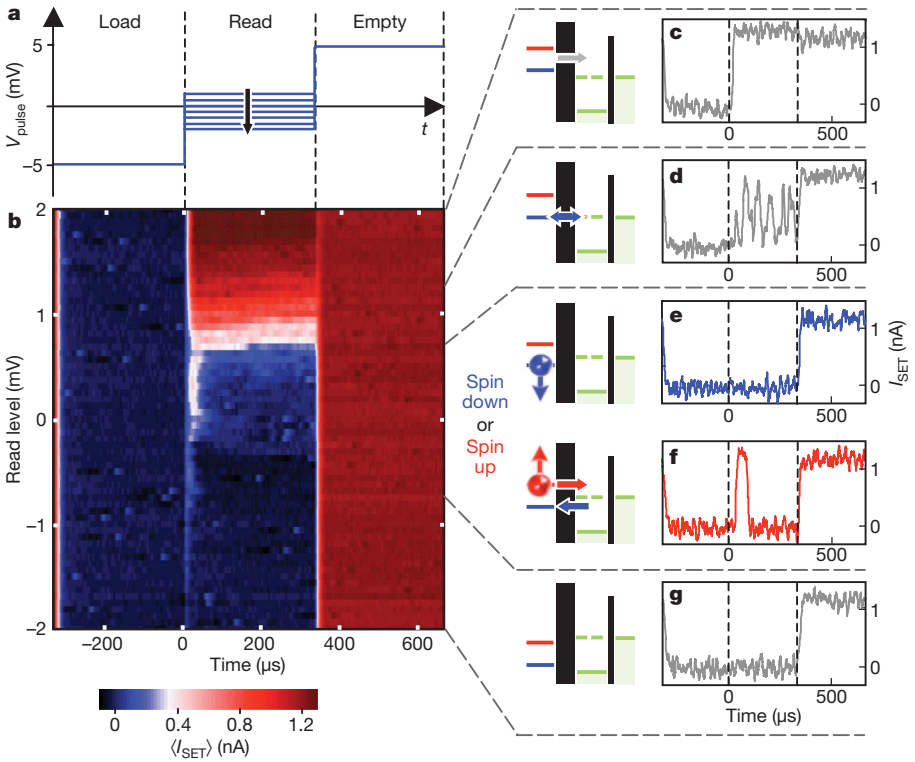

Figure 2 | Single-shot spin readout and calibration of the 'read' level. **a**, Three-level pulsing sequence for spin readout. The 'load' and 'empty' levels are kept constant, while the read level is scanned from high to low. **b**, SET current $\langle I_{SET}\rangle$, averaged over 128 single-shot traces (colour scale), as a function of the V_{pulse} level during the read phase. Data taken with an applied magnetic field $B = 5$ T and a detection bandwidth of 40 kHz (rise time ~10 μs). **c**–**g**, Examples of single-shot traces. **c**, Read level too high, $\mu_\downarrow > \mu_{SET}$: the electron always leaves the donor during the read pulse, regardless of its spin. **d**, $\mu_\downarrow \approx \mu_{SET}$: random telegraph signal indicates an electron switching between SET island and $|\downarrow\rangle$ state. **e**, **f**, Correct read level, $\mu_\downarrow < \mu_{SET} < \mu_\uparrow$: $I_{SET} = 0$ during the read phase indicates a $|\downarrow\rangle$ state (**e**). A single current pulse at the beginning of the read phase is the signature of a $|\uparrow\rangle$ state (**f**). The regime of correct read level is recognizable by the isolated increase in $\langle I_{SET}\rangle$ in **b**. **g**, Read level too low, $\mu_\uparrow < \mu_{SET}$: the electron never leaves the donor during the read pulse.

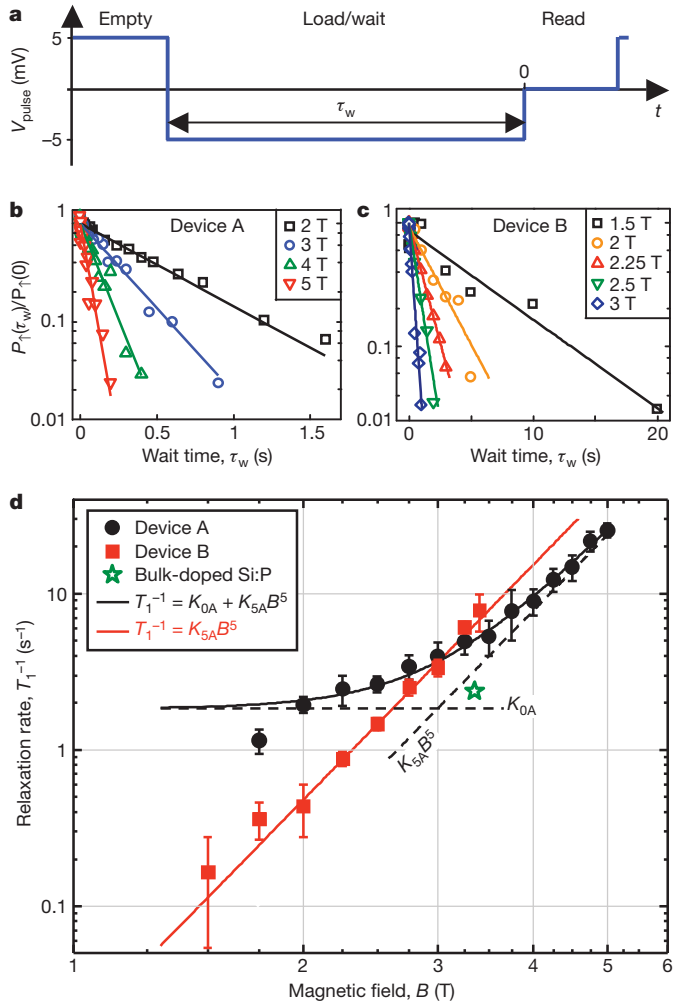

Figure 3 | Spin relaxation rate. **a**, Pulsing sequence for measuring the spin relaxation rate $1/T_1$, identical to Fig. 1b but with a variable load/wait time, τ_w. **b**, **c**, Exponential decays of the normalized spin-up fraction at different magnetic fields, for devices A and B as indicated. **d**, Magnetic field dependence of T_1^{-1}. Error bars, 95% confidence levels. The data for device A follow $T_1^{-1} = 1.84\,s^{-1} + 0.0076B^5\,s^{-1}\,T^{-5}$ (black solid line, sum of the dashed lines). The point at $B = 1.75$ T is not included in the fitted data set. The data for device B follow $T_1^{-1} = 0.015B^5\,s^{-1}\,T^{-5}$ (red line). The star is a data point measured on a bulk Si:P crystal at $T < 5$ K (J. J. L. Morton, personal communication).

To assess the effectiveness of the spin readout process for quantum information purposes, it is important to quantify the readout fidelity, that is, the probability that an electron spin state is recognized correctly. In Fig. 4, we show the analysis of the readout fidelity for a set of 10,000 traces. The spin state is declared $|\uparrow\rangle$ if the peak value I_p taken by $I_{SET}(t)$ in the interval $0 < t < 100\ \mu s$ surpasses the threshold current I_T, and $|\downarrow\rangle$ otherwise. The probability distribution of I_p (Fig. 4b) shows well-resolved peaks, indicating that I_p takes two preferential values depending on the electron spin state. We have developed a numerical model that accurately simulates the measurement process and yields two separate histograms of peak current values for the states $|\downarrow\rangle$ and $|\uparrow\rangle$, $N_{\downarrow,\uparrow}(I_p)$, respectively (Supplementary Information). The calculated $N_{\downarrow,\uparrow}(I_p)$ are in excellent agreement with the measured histogram (Fig. 4b).

With the knowledge of $N_{\downarrow,\uparrow}(I_p)$, the readout fidelities[15] are obtained as $F_\downarrow = 1 - \int_{I_T}^{\infty} N_\downarrow(I)\mathrm{d}I$ and $F_\uparrow = 1 - \int_{-\infty}^{I_T} N_\uparrow(I)\mathrm{d}I$ for the states $|\downarrow\rangle$ and $|\uparrow\rangle$, respectively, as a function of the discrimination threshold I_T (Fig. 4c).

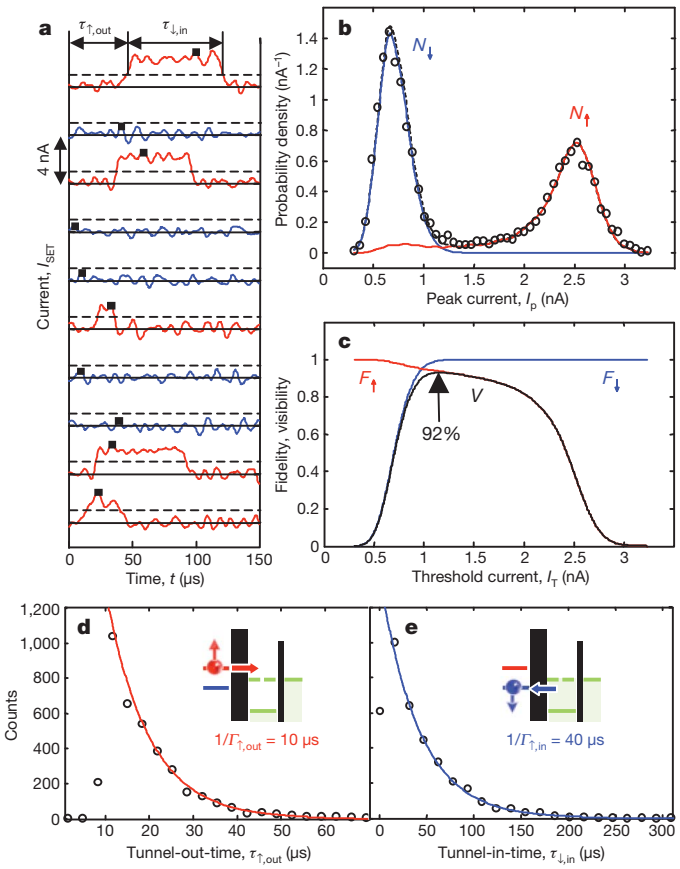

Figure 4 | Readout fidelity and visibility. **a**, Examples of single-shot I_{SET} traces, each shifted by 4 nA for clarity, with $B = 5$ T and 120 kHz bandwidth (~3 μs rise/fall time). The spin is labelled $|\uparrow\rangle$ (red trace) or $|\downarrow\rangle$ (blue trace), depending on whether I_{SET} passes the threshold $I_T = 1.1$ nA (dashed lines). **b**, Histogram (circles) of the maximum values of I_{SET} in the interval $0 < t < 100\ \mu s$ (black squares in **a**), obtained from a 10,000-shots data set. The blue and red lines are simulated histograms for states $|\downarrow\rangle$ and $|\uparrow\rangle$, respectively, and the black dashed line is the sum of the two. The simulated curves are obtained using $P_\uparrow = 0.47$, $\Delta I = 1.9$ nA, $1/\Gamma_{\uparrow,out} = 10\ \mu s$, $1/\Gamma_{\downarrow,in} = 40\ \mu s$. **c**, $|\downarrow\rangle$ (blue) and $|\uparrow\rangle$ (red) readout fidelities, and readout visibility (black) as a function of the discrimination threshold, I_T. The maximum visibility is 92% at $I_T \approx 1.1$ nA. **d**, **e**, Histogram (circles) of the tunnel-out times for spin-up electrons, $\tau_{\uparrow,out}$ (**d**), and subsequent tunnel-in times for spin-down electrons, $\tau_{\downarrow,in}$ (**e**), as defined on the top trace in **a**. In **d**, we note a systematic ~10 μs delay between the beginning of the read phase and the tunnel-out events, due to the response of the amplifier and filter chain. The solid lines are exponential fits to extract the tunnel rates. These values of $1/\Gamma_{\uparrow,out}$ and $1/\Gamma_{\downarrow,in}$ were used to obtain the simulated curves in **b**.

The integrals in $F_{\downarrow,\uparrow}$ represent the probability that the spin state is incorrectly assigned, either because a spin-down trace has a noise spike $> I_T$, or because a spin-up signal does not reach the threshold. The visibility, defined as $V = F_\downarrow + F_\uparrow - 1$, reaches a maximum value of ~92% at $I_T = 1.1$ nA, where the readout fidelities are $F_\downarrow \approx 99\%$ and $F_\uparrow \approx 93\%$.

Combining spin resonance experiments[11,30] with the ability to read out a single spin will provide a promising system in which to demonstrate and exploit coherent quantum control of a donor electron and nuclear spin. The high-fidelity, single-shot electron spin readout, demonstrated here for the first time in silicon, represents an important step towards unlocking the full potential of silicon-based quantum information science and technology.

METHODS SUMMARY

The devices were fabricated on a high-purity, near-intrinsic, natural-isotope (100) silicon substrate, with n^+ ohmic source/drain contacts obtained by phosphorus diffusion. A high-quality SiO_2 gate oxide was grown by dry oxidation at 800 °C, with thicknesses of 5 nm (device A) or 10 nm (device B). Phosphorus ions were implanted through a 90 nm × 90 nm aperture defined by electron-beam lithography in a poly (methyl methacrylate) mask. The chosen fluence maximizes the likelihood of having three P atoms in a 30 nm × 30 nm area, subject to Poisson statistics. The implantation energy was 14 keV, resulting in an average depth of ~15 nm (device A) or ~10 nm (device B) below the Si/SiO_2 interface. A 5 s, 1,000 °C rapid thermal anneal was performed to activate the donors and repair the implantation damage. The aluminium gates to form the SET were defined by electron-beam lithography, followed by Al thermal evaporation and lift-off. A final forming gas anneal (400 °C, 15 min, 95% N_2 / 5% H_2) was performed to reduce the interface trap density to the level of 2×10^{10} cm^{-2} eV^{-1}, as measured on devices fabricated with the same process.

The sample was mounted on a high-frequency printed circuit board in a copper enclosure, and thermally anchored to the cold finger of a dilution refrigerator with base temperature ~40 mK. Semirigid coaxial lines, fitted with copper-powder filters at the base temperature plus *RC*-filters on the circuit board, connected the sample to the room-temperature electronics. All d.c. voltages to the gates were provided by optoisolated and battery-powered voltage sources, and added through resistive voltage dividers/combiners to the pulses produced by an arbitrary waveform generator. The SET current was measured by a room-temperature transimpedance amplifier, followed by a voltage post-amplifier, an eighth-order low-pass Bessel filter, and a fast digitizing oscilloscope.

Received 28 April; accepted 2 August 2010.
Published online 26 September 2010.

1. Levi, A. J. F. Towards quantum engineering. *Proc. IEEE* **96,** 335–342 (2008).
2. Loss, D. & DiVincenzo, D. P. Quantum computation with quantum dots. *Phys. Rev. A* **57,** 120–126 (1998).
3. Kane, B. E. A silicon-based nuclear spin quantum computer. *Nature* **393,** 133–137 (1998).
4. Hollenberg, L. C. L., Greentree, A. D., Fowler, A. G. & Wellard, C. J. Two-dimensional architectures for donor-based quantum computing. *Phys. Rev. B* **74,** 045311 (2006).
5. Žutić, I., Fabian, J. & Das Sarma, S. Spintronics: fundamentals and applications. *Rev. Mod. Phys.* **76,** 323–410 (2004).
6. Tyryshkin, A. M., Lyon, S. A., Astashkin, A. V. & Raitsimring, A. M. Electron spin relaxation times of phosphorus donors in silicon. *Phys. Rev. B* **68,** 193207 (2003).
7. Feher, G. & Gere, E. A. Electron spin resonance experiments on donors in silicon. II. Electron spin relaxation effects. *Phys. Rev.* **114,** 1245–1256 (1959).
8. Ager, J. W. *et al.* High-purity, isotopically enriched bulk silicon. *J. Electrochem. Soc.* **152,** G448–G451 (2005).
9. Jamieson, D. N. *et al.* Controlled shallow single-ion implantation in silicon using an active substrate for sub-20-keV ions. *Appl. Phys. Lett.* **86,** 202101 (2005).
10. Angus, S. J., Ferguson, A. J., Dzurak, A. S. & Clark, R. G. Gate-defined quantum dots in intrinsic silicon. *Nano Lett.* **7,** 2051–2055 (2007).
11. Morello, A. *et al.* Architecture for high-sensitivity single-shot readout and control of the electron spin of individual donors in silicon. *Phys. Rev. B* **80,** 081307(R) (2009).
12. Ladd, T. D. *et al.* Quantum computers. *Nature* **464,** 45–53 (2010).
13. Elzerman, J. M. *et al.* Single-shot read-out of an individual electron spin in a quantum dot. *Nature* **430,** 431–435 (2004).
14. Hanson, R. *et al.* Single-shot readout of electron spin states in a quantum dot using spin-dependent tunnel rates. *Phys. Rev. Lett.* **94,** 196802 (2005).
15. Barthel, C., Reilly, D. J., Marcus, C. M., Hanson, M. P. & Gossard, A. C. Rapid single-shot measurement of a singlet-triplet qubit. *Phys. Rev. Lett.* **103,** 160503 (2009).
16. Devoret, M. H. & Schoelkopf, R. J. Amplifying quantum signals with the single-electron transistor. *Nature* **406,** 1039–1046 (2000).
17. Goswami, S. *et al.* Controllable valley splitting in silicon quantum devices. *Nature Phys.* **3,** 41–45 (2007); published online 10 December 2006..
18. Morton, J. J. L. *et al.* Solid-state quantum memory using the ^{31}P nuclear spin. *Nature* **455,** 1085–1088 (2008).

19. Hofmann, F. *et al.* Single electron switching in a parallel quantum dot. *Phys. Rev. B* **51,** 13872–13875 (1995).
20. Huebl, H. *et al.* Electron tunnel rates in a donor-silicon single electron transistor hybrid. *Phys. Rev. B* **81,** 235318 (2010).
21. Tan, K. Y. *et al.* Transport spectroscopy of single phosphorus donors in a silicon nanoscale transistor. *Nano Lett.* **10,** 11–15 (2010).
22. DiVincenzo, D. P. The physical implementation of quantum computation. *Fortschr. Phys.* **48,** 771–783 (2000).
23. Hanson, R., Kouwenhoven, L. P., Petta, J. R., Tarucha, S. & Vandersypen, L. K. Spins in few-electron quantum dots. *Rev. Mod. Phys.* **79,** 1217–1265 (2007).
24. Hasegawa, H. Spin-lattice relaxation of shallow donor states in Ge and Si through a direct phonon process. *Phys. Rev.* **118,** 1523–1534 (1960).
25. Hayes, R. R. *et al.* Lifetime measurements (T_1) of electron spins in Si/SiGe quantum dots. Preprint at ⟨http://arxiv.org/abs/0908.0173⟩ (2009).
26. Xiao, M., House, M. G. & Jiang, H. W. Measurement of the spin relaxation time of single electrons in a silicon metal-oxide-semiconductor-based quantum dot. *Phys. Rev. Lett.* **104,** 096801 (2010).
27. de Sousa, R. Dangling-bond spin relaxation and magnetic 1/f noise from the amorphous-semiconductor/oxide interface: theory. *Phys. Rev. B* **76,** 245306 (2007).
28. Shankar, S., Tyryshkin, A. M., He, J. & Lyon, S. A. Spin relaxation and coherence times for electrons at the Si/SiO_2 interface. Preprint at ⟨http://arxiv.org/abs/0912.3037⟩ (2009).
29. Calderón, M. J., Saraiva, A., Koiller, B. & Das Sarma, S. Quantum control and manipulation of donor electrons in Si-based quantum computing. *Appl. Phys. Lett.* **105,** 122410 (2009).
30. Xiao, M., Martin, I., Yablonovitch, E. & Jiang, H. W. Electrical detection of the spin resonance of a single electron in a silicon field-effect transistor. *Nature* **430,** 435–439 (2004).

Supplementary Information is linked to the online version of the paper at www.nature.com/nature.

Acknowledgements We thank D. D. Awschalom, C. Tahan, J. J. L. Morton and G. Prawiroatmodjo for comments and suggestions, W. H. Lim for assistance with device fabrication, and R. P. Starrett, D. Barber, A. Cimmino and R. Szymanski for technical assistance. We acknowledge support from the Australian Research Council, the Australian Government, the US National Security Agency and the US Army Research Office under contract number W911NF-08-1-0527. M.M. acknowledges support from the Academy of Finland and the Emil Aaltonen foundation.

Author Contributions A.M., H.H., C.D.N., D.N.J., C.C.E., L.C.L.H., R.G.C. (while at UNSW) and A.S.D. conceived and designed the experiment, K.W.C. and K.Y.T. fabricated the devices, C.Y., J.A.v.D., A.D.C.A. and D.N.J. implanted the P donors, A.M., J.J.P. and F.A.Z. performed and analysed the measurements, A.M., M.M. and J.J.P. analysed the readout fidelity. A.M. wrote the manuscript with input from all coauthors.

Author Information Reprints and permissions information is available at www.nature.com/reprints. The authors declare no competing financial interests. Readers are welcome to comment on the online version of this article at www.nature.com/nature. Correspondence and requests for materials should be addressed to A.M. (a.morello@unsw.edu.au).